

Dative and Electron-Sharing Bonding in C₂F₄

Diego M. Andrada,^{a,b} José Luis Casalz-Sainz,^c Ángel Martín Pendas,^{*c} and Gernot Frenking^{*a,d}

^aFachbereich Chemie, Philipps-Universität Marburg, Hans-Meerwein-Straße, 35043 Marburg, Germany

^bPresent address: Institut für Allgemeine und Anorganische Chemie, Universität des Saarlandes, D-66123 Saarbrücken, Germany

^cDepartment of Analytical and Physical Chemistry, University of Oviedo, E-33006 Oviedo, Spain.

^dInstitute of Advanced Synthesis, Nanjing Tech University, 211816 Nanjing, China

Abstract. The reaction pathway for the rupture of the carbon-carbon double bond of C₂F₄ has been calculated with *ab initio* methods at the CASSCF(8,8)+NEVPT2/aug-cc-pVTZ and CCSD(T)/aug-cc-pVTZ levels and with density functional theory using M06-L and M06-2X functionals in conjunction with aug-cc-pVTZ basis sets. The calculations suggest that the bond dissociation pathway proceeds via a nonlinear reaction course without activation barrier yielding the CF₂ fragments in the (¹A₁) ground state. A bonding analysis indicates that there is a continuous change in the electronic structure of the CF₂ fragments during the elongation of the C-C distance from a (³B₁) excited state at the equilibrium geometry of C₂F₄ to the (¹A₁) ground state. EDA-NOCV calculations suggest that the carbon-carbon interactions in C₂F₄ at equilibrium distance and longer C-C values up to ~1.60 Å are best described in terms of electron-sharing bonding between the CF₂ fragments in the (³B₁) excited state. At longer distances, the situation changes toward dative bonding between CF₂ fragments in the (¹A₁) ground state.

Introduction

The bond dissociation energy (BDE) of the carbon-carbon double bond in tetrafluoroethylene is a striking example of the failure of using thermodynamic data for estimating the strength of a chemical bond. The C-C bond energy of $\text{F}_2\text{C}=\text{CF}_2$ is only 70.3 kcal/mol, much lower than the C-C bond energy of $\text{H}_2\text{C}=\text{CH}_2$ (172.1 kcal/mol) and even lower than the bond energy of the C-C single bond in $\text{F}_3\text{C}-\text{CF}_3$ (96.4 kcal/mol).^[1] The BDE values are also evidence against a naive correlation of bond lengths and energy data. The carbon-carbon bond length in C_2F_4 (1.311 Å) is even shorter than in C_2H_4 (1.336 Å) and much shorter than in C_2F_6 (1.545 Å).^[2] Carter and Goddard^[3] explained the small BDE of C_2F_4 with the rather large excitation energy of 54 ± 3 kcal/mol^[4] of the singlet ($^1\text{A}_1$) electronic ground state of CF_2 to the triplet ($^3\text{B}_1$) excited state, which is the electronic reference state of the CF_2 fragments in C_2F_4 (Figure 1). Unlike CF_2 , methylene CH_2 has a triplet ($^3\text{B}_1$) ground state, which is perfectly suited for the formation of an electron-sharing double bond in $\text{H}_2\text{C}=\text{CH}_2$. The singlet ($^1\text{A}_1$) excited state of CH_2 is 9.0 kcal/mol higher in energy than the ground state.^[5]

Figure 1

The dissociation of C_2F_4 into two CF_2 fragments in the ($^1\text{A}_1$) ground state was already discussed in 1968 by Simons^[6] using a correlation diagram where the ($^3\text{B}_1$) excited state and the ground state of CF_2 are crossing along the reaction pathway, which was assumed to be non-linear. It follows that the CF_2 moieties in an early stadium of the bond formation engage in dative interactions in their ($^1\text{A}_1$) ground state (Figure 2b). At some point of the association pathway, the interactions are then better described in terms of electron-sharing double bonds between the CF_2 fragments in the ($^3\text{B}_1$) excited state, which is the appropriate description in the planar (D_{2h}) equilibrium structure (Figure 2a). It is interesting to note that the heavier group-14 homologues of ethylenes E_2R_2 (E = Si - Pb) with various substituents R "get stuck" along the association pathway between the ER_2 fragments and retain a trans-bent equilibrium geometry.^[7] Malrieu and Trinquier showed that the trans-bent equilibrium geometries of the latter species may be discussed in terms of dative bonds as shown in Figure 2b.^[8]

Figure 2

To the best of our knowledge, the actual dissociation pathway for the reaction $\text{C}_2\text{F}_4 \rightarrow 2 \text{CF}_2$ has not been calculated before, nor was the change in the bonding situation during the reaction studied. According to the suggested bonding models in Figure 2, there should be a transition from electron-sharing double bonds to dative bonds during the fragmentation of the C-C bond in C_2F_4 . This can be monitored by an energy decomposition analysis (EDA) of C_2F_4 along the dissociation pathway, where CF_2 in the ($^3\text{B}_1$) triplet state and ($^1\text{A}_1$) singlet state are taken as interacting fragments. We have shown in several studies that the strength of the orbital interactions between the fragments in different electronic states is a useful indicator for the best description of the chemical bond.^[9] Those fragments, which yield the smallest orbital interaction energy, indicate the most faithful model for the bonding situation. This was particularly useful in cases where the description in terms of dative bonds $\text{A} \rightarrow \text{B}$ or electron-sharing bonds $\text{A}-\text{B}$ was not clear.^[9c,g,]

In this work, we present the calculated dissociation pathway for the reaction $\text{C}_2\text{F}_4 \rightarrow 2 \text{CF}_2$ using multireference *ab initio* methods and density functional theory (DFT) and we discuss the nature of the bonding situation along the reaction course. The alteration of the electronic structure is monitored with the EDA method developed by Ziegler and Rauk.^[10]

Methods

The calculations were done as follow. First we carried out a preoptimization of the path with the only geometrical restriction of the C-C distance using density functional theory (DF) with the meta generalized gradient (MGG) M06-L functional^[11] in conjunction with aug-cc-pvTZ^[12] basis sets. The resulting set of point, which were optimized without symmetry constraints, gave a path belonging to the C_{2h} point group at large distances and D_{2h} at short distances. Then we calculated a second pathway with shorter intervals between those points where a deviation from a planar structure was observed. In order to follow the same path we have used the C_{2h} point group in all points except close to the equilibrium region, since C_{2h} is a subgroup of D_{2h} . This allows us to get a smooth transition near the region in which the molecule adopts a quasi D_{2h} point group. The resulting energy path parallels the energy and geometries obtained in the original C_1 scan. With this final set of geometries we

calculated the energies along the dissociation path with various methods. The methods used besides the original M06-L are CCSD^[13], CCSD(T)^[14], M06-2X^[15], CASSCF(8,8)^[16] and CASSCF(8,8)+NEVPT2^[17]. In the CCSD and CCSD(T) calculations, only valence electrons were correlated. For the CASSCF(8,8) calculations we used a modified AVAS^[18] technique (core orbitals are excluded from the projecting step and a splitting of the threshold for the occupied and virtual set was implemented) to select the orbital space. In all cases we used the orbitals from the equilibrium distance and propagated them during the scan, using as impurities the σ and π orbitals. The electronic state was in all cases the totally symmetric representation of the corresponding point group. The resulting space is composed of 8 electrons in 8 orbitals where 4 of them are the bonding/antibonding σ and π orbitals and the rest come from p_y orbitals of F (the y axis is perpendicular to the C-C bond, so F(p_y) orbitals possess π symmetry). Using the CASSCF(8,8) guesses we also performed NEVPT2 calculations at each point, correlating all electrons including core electrons.

The calculations for the bonding analysis were performed using the M06-L/aug-cc-pVTZ optimized structures along the dissociation pathway. The atomic partial charges were calculated with the natural bonds orbital (NBO) method of Weinhold and Landis^[19] using NBO 3.1. The Wiberg bond orders^[20] were also computed at M06-L/aug-cc-pVTZ using the program package Gaussian 09.^[21]

. The nature of the carbon-carbon interactions was investigated with the EDA (energy decomposition analysis) of Ziegler and Rauk.^[10] The EDA focuses on the instantaneous interaction energy ΔE_{int} of the chemical bonds between two or more fragments in the particular electronic reference state and in the frozen geometry of the molecule.^[22] The interaction energy ΔE_{int} is divided into three main components [Eq. (1)].

$$\Delta E_{\text{int}} = \Delta E_{\text{elstat}} + \Delta E_{\text{Pauli}} + \Delta E_{\text{orb}} \quad (1)$$

The term ΔE_{elstat} corresponds to the quasiclassical electrostatic interaction between the unperturbed charge distributions of the prepared atoms and is usually attractive. The Pauli repulsion ΔE_{Pauli} is the energy change associated with the transformation from the superposition of the unperturbed electron densities $\rho_A + \rho_B$ of the isolated fragments to the wavefunction $\Psi^0 = N\hat{A}[\Psi_A\Psi_B]$, which properly obeys the Pauli principle through explicit

antisymmetrization (\hat{A} operator) and renormalization ($N = \text{constant}$) of the product wavefunction. ΔE_{Pauli} comprises the destabilizing interactions between electrons of the same spin on either fragment. The orbital interaction ΔE_{orb} , which accounts for charge transfer and polarization effects, indicates the total change in the electronic structure that is associated with the bond formation.

The EDA calculations were carried out with program package ADF2016²³ using the M06-L functional in conjunction with uncontracted Slater-type orbitals (STOs)²⁴ with TZ2P quality as basis functions. The latter basis sets have triple- ζ quality augmented by two sets of polarization functions. An auxiliary set of s, p, d, f, and g STOs was used to fit the molecular densities and to represent the Coulomb and exchange potentials accurately in each SCF cycle.²⁵ The EDA calculations at M06-L/TZ2P level were performed using M06-L/aug-cc-pVTZ optimized geometries. Since M06-L is employed, the MGG expression $\Delta E_{\text{MetaGGA}}$ becomes an additional term in equation (1).

Results and Discussion

Table 1 shows the calculated C-C distances and bond dissociation energies (BDEs) of the hydrogen and fluorine substituted ethanes and ethenes at the M06-L/TZ2P level of theory. The theoretical data are in very good agreement with experimental results.^[2] They confirm the surprisingly small BDE of C₂F₄.

Table 1

Figure 3 shows the calculated dissociation pathway for breaking the C-C bond of C₂F₄ at different levels of theory. The single point energies at 0.1 Å intervals of the C-C bond length at the CASSCF(8,8)+NEVPT2/aug-cc-pVTZ level of theory using M06-L/aug-cc-pVTZ optimized geometries with frozen C-C distances suggest that there is a smooth dissociation from C₂F₄ to two CF₂ fragments in the (¹A₁) ground state. The planar D_{2h} equilibrium structure becomes distorted toward a trans-bent F₂C \cdots CF₂ geometry at longer distances, which agrees with the crossing of two electronic states of CF₂ along the potential energy curve proposed by Simons.^[6] Note that the energy curve at the CASSCF(8,8) /aug-cc-pVTZ level exhibits a small hump at d_{C-C} ~ 2.2 Å, which disappears when dynamical

correlation is considered at CASSCF(8,8)+NEVPT2/aug-cc-pVTZ. It is noteworthy that the single-configuration calculations at CCSD(T)/aug-cc-pVTZ and the DFT calculations at M06-L/aug-cc-pVTZ and M06-L/aug-cc-pVTZ give very similar energy curves as the CASSCF(8,8)+NEVPT2/aug-cc-pVTZ values. The results suggest that the dissociation reaction $C_2F_4 \rightarrow 2 CF_2$ proceeds via a nonplanar pathway without a barrier yielding difluorocarbene molecules in the (1A_1) ground state.

Figure 3, Table 2

Table 2 gives the relative energies of C_2F_4 for different C-C distances at the theoretical methods that were used. It gives also the bending angle α of the CF_2 groups, which indicates the deviation from D_{2h} symmetry. It becomes obvious that stretching of the C-C distance from the equilibrium distance of 1.326 Å to $d_{C-C} = 1.50$ Å leads already to a bending angle of 21.8° and that the largest value at long C-C distances is ~ 62°. Looking in the reverse direction, the approach of the CF_2 groups during the formation of the C=C double bond is perfectly suited for cooperative dative bonding as shown in Figure 2b. The bonding model **B** for donor-acceptor interaction between the CF_2 groups in the (1A_1) ground state appears as the best representation for the bonding situation at an early stadium of the bond formation. The final point is C_2F_4 at the equilibrium structure, which may be described with electron-sharing σ and π bonds between two CF_2 fragments in the (3B_1) excited state as in model **A** (Figure 2a). Alternatively, C_2F_4 may still be written at the equilibrium structure with dative bonds where one CF_2 is in the highly excited (1B_1) state (Bonding model **C**, Figure 2c). In any case, there is a change in the bonding situation during bond formation either from **A** \rightarrow **B** or **A** \rightarrow **C**.

The alteration in the electronic structure of C_2F_4 along the reaction course and the question about the best bonding model can be addressed with EDA calculations using the CF_2 fragments with different electronic states as interacting species. As noted above, the absolute value of the ΔE_{orb} value indicates the best choice of the fragments and thus, the most appropriate type of interaction for describing the bonding situation. Those fragments who energetically change least are considered as the most faithful model for the interacting species. Table 3 gives the ΔE_{orb} values at the M06-L/TZ2P+ level of theory. The full set of numerical EDA results is given in Table S1 (Supporting Information).

Table 3

The data in Table 3 show that the interactions between CF₂ in the (³B₁) excited state (bonding model **A**) give the smallest ΔE_{orb} values at the equilibrium distance of C₂F₄ and at longer C-C distances up to 1.60 Å. When the C-C bond is stretched to 1.70 Å and longer, the smallest ΔE_{orb} values are found for the interactions between the (¹A₁) ground state of CF₂ (bonding model **B**). The EDA calculations indicate that bonding model **C** is not a valid description at any C-C distance. The oscillation of the ΔE_{orb} values when one uses model **C** between 1.40 Å and 1.70 Å show that the approach using different electronic states of the fragments is no reasonable description of the bond rupture. But the trend of the ΔE_{orb} values at different C-C distances appears as a faithful gauge for the change in the bonding situation. The numerical data for models **A** and **B** clearly indicate which bonding model is more appropriate for describing the C-C interactions at different C-C distances.

Table 4

Table 4 gives the numerical EDA-NOCV results for C₂H₄ and C₂F₄ at the equilibrium distances using singlet and triplet carbene fragments as interacting species. As expected, the ΔE_{orb} values suggest that the description with electron-sharing σ and π bond is the appropriate model for the bonding situation. The intrinsic interaction energy ΔE_{int} between the fragments in the (³B₁) state in ethylene (-196.7 kcal/mol) is slightly smaller than in tetrafluoroethylene (-197.7 kcal/mol). The covalent (orbital) interactions ΔE_{orb} in C₂H₄ provide 63 % to the total attraction and 64 % in C₂F₄. The C-C σ bond in C₂H₄ amounts to 70 % of the covalent interactions and the π bond contributes 25 %. The remaining 5% comes from weak intra- and interorbital interactions. Similar values are calculated for C₂F₄, where the C-C σ bond provides 64 % to the covalent interaction while the π bond contributes 27 %. The numerical values of the EDA-NOCV calculations suggest that the carbon-carbon bonds in C₂H₄ and C₂F₄ are very similar to each other.

Figure 4

Figure 4 displays the deformation densities Δρ, which are associated with the formation of the C-C σ and π bonds of the two molecules. There is charge accumulation in the σ and π space of the interatomic bonding region and charge depletion in the valence space close to the atomic region of carbon. The shape Δρ(σ) of C₂F₄ reveals that the formation of the C-C σ bond leads also to a charge migration at the fluorine atoms toward the carbon-fluorine bonding region. This agrees with the calculated shortening of the C-F distance of

1.314 Å in CF₂ (³B₁) to 1.312 Å in C₂F₄. In contrast, the C-H bond length in CH₂ (³B₁) is clearly shorter (1.074 Å) than in C₂H₄ (1.082 Å).

The electron density itself also shows clear indications of the electron-sharing to dative bonding transition. Figure 5 displays the evolution of the -0.2 au isosurface of the Laplacian of the density during the rupture of the C-C bond. $\nabla^2\rho$ changes from negative (shared-shell interaction) to positive in the CF₂ inter-fragment region during bond cleavage. In this process, progress toward model **B** as well as the formation of the CF₂ lone pairs is strikingly visible. A similar image can be obtained from Figure 6, which shows the bonding natural adaptive orbitals (NAdOs)^[26] between the two CF₂ fragments along the dissociation. NAdOs provide a partitioning of the shared-electron bond order into orbital contributions. Two bonding terms dominate at all distances that change continuously from a σ - π distribution at equilibrium to the dative bonding situation at larger distances.

Figure 5

Figure 6

The results of this work suggest a cautionary detail to be considered for the definition of a dative bond, which is given by the IUPAC. The IUPAC rules state that "The distinctive feature of dative bonds is that their minimum-energy rupture in the gas phase or in inert solvent follows the heterolytic bond cleavage path."^[27] The bonding analysis of C₂F₄ clearly shows that the molecule has an electron-sharing C=C double bond, which changes toward $C\rightleftharpoons C$ dative bonding during bond cleavage. While the rupture of dative bonds takes place via a heterolytic bond cleavage path, the reverse conclusion may not be justified. Heterolytic bond cleavage is not a definite criterion for dative bonding.

Summary and Conclusion

The results of this work may be summarized as follows. The bond dissociation pathway for rupture of the carbon-carbon double bond of C₂F₄ proceeds via a nonlinear course without activation barrier yielding the CF₂ fragments in the (¹A₁) ground state. There is a continuous change in the electronic structure of the CF₂ fragments during the elongation of the C-C

distance from a (3B_1) excited state at the equilibrium geometry of C_2F_4 to the (1A_1) ground state. The EDA-NOCV calculations suggest that the carbon-carbon interactions in C_2F_4 at equilibrium distance and longer C-C values up to ~ 1.60 Å are best described in terms of electron-sharing bonding between the CF_2 fragments in the (3B_1) excited state. At longer distances, the situation changes toward dative bonding between CF_2 fragments in the (1A_1) ground state. The transition is easily followed by examining the evolution of the Laplacian of the electron density or the shape of the bonding natural adaptive orbitals.

References

- 1 Values are calculated from the experimental data of the heats of formation of C₂F₄ (-157.3 kcal/mol), CF₂ (-43.5 kcal/mol), C₂F₆ (-321.0 kcal/mol), CF₃ (-112.3 kcal/mol), C₂H₄ (12.5 kcal/mol), CH₂ (92.3 kcal/mol), C₂H₆ (-20.1 kcal/mol), CH₃ (34.8 kcal/mol),. The data are taken from the NIST Chemistry Webbook, SRD 69: <http://webbook.nist.gov/chemistry/>.
- 2 Experimental gas phase values of the C-C bonds. a) C₂F₄: J. L. Carlos, R. R. Karl, S. H. Bauer, *J. Chem. Soc. Farad. Trans. II*, **1974**, *70*, 177-187; b) C₂H₄: L. S. Bartell, E. A. Roth, C. D. Hollowell, K. Kuchitsu, J. E Young, *J. Chem. Phys.*, **1965**, *42*, 2683-2686; c) C₂F₆ K. L. Gallaher, A. Yokozeki, S. H Bauer, *J. Phys. Chem.*, **1974**, *78*, 2389- 2395; d) C₂H₆: M. D. Harmony, *J. Chem. Phys.* **1990**, *93*, 7522-7523.
- 3 E. A. Carter, W. A. Goddard, *J. Phys. Chem.* **1986**, *90*, 998-1001.
- 4 R. L. Schwartz, G. E. Davico, T. M. Ramond, W. C. Lineberger, *J. Phys. Chem. A* **1999**, *103*, 8213-8221.
- 5 a) A. R. W. McKellar, P. R. Bunker, T. J. Sears, K. M. Evenson, R. J. Saykally, S. R. Langhoff, *J. Chem. Phys.* **1983**, *79*, 5251-5164; b) D. G. Leopold, K. K. Murray, W. C. Lineberger, *J. Chem. Phys.* **1984**, *81*, 1048-1050; c) D. G. Leopold, K. K. Murray, A. E. S. Miller, W. C. Lineberger, *J. Chem. Phys.* **1985**, *83*, 4849-4865; d) P. R. Bunker, T. J. Sears, *J. Chem. Phys.* **1985**, *83*, 4866-4876.
- 6 J. P. Simons, *Nature* **1965**, *205*, 1308-1309.
- 7 P. Chakkingal, R. Hoffmann, *Organometallics* **2017**, *36*, 4825-4833.
- 8 G. Trinquier, J.-P. Malrieu, *J. Am. Chem. Soc.* **1989**, *111*, 5916-5921.
- 9 Recent representative studies: a) Q. Zhang, W.-L. Li, C. Xu, M. Chen, M. Zhou, J. Li, D. M. Andrada, G. Frenking, *Angew. Chem. Int. Ed.* **2015**, *54*, 11078-11083; *Angew. Chem.* **2015**, *127*, 11230-11235; b) D. M. Andrada, G. Frenking, *Angew. Chem. Int. Ed.* **2015**, *54*, 12319-12324; *Angew. Chem.* **2015**, *127*, 12494-12499; c) C. Mohapatra, S. Kundu, A. N. Paesch, R. Herbst-Irmer, D. Stalke, D. M. Andrada, G. Frenking, H. W. Roesky, *J. Am. Chem. Soc.* **2016**, *138*, 10429-10432; d) Z. Li, X. Chen, D. M. Andrada, G. Frenking, Z. Benkő, Y. Li, J. Harmer, C.-Y. Su, H. Grützmacher, *Angew. Chem. Int.*

-
- Ed.* **2017**, *56*, 5744-5749; *Angew. Chem.* **2017**, *129*, 5838-5843; e) L. T. Scharf, M. Andrada, G. Frenking, V. H. Gessner, *Chem. Eur. J.* **2017**, *23*, 4422-4434; f) M. Hermann, G. Frenking, *Chem. Eur. J.* **2017**, *23*, 3347-3356; g) D. C. Georgiou, L. Zhao, D. J. D. Wilson, G. Frenking, J. L. Dutton, *Chem. Eur. J.* **2017**, *23*, 2926-34. h) L. Zhao, M. Hermann, N. Holzmann, G. Frenking, *Coord. Chem. Rev.* **2017**, *344*, 163-204.
- 10 a) T. Ziegler, A. Rauk, *Inorg. Chem.* **1979**, *18*, 1755-1759. b) T. Ziegler, A. Rauk, *Inorg. Chem.* **1979**, *18*, 1558-1565.
- 11 Y. Zhao, D. G. Truhlar, *J. Chem. Phys.* **2006** *125*, 194101-194118.
- 12 K. E. Yousaf, K. A. Peterson, *Chem. Phys. Lett.* **2009**, *476*, 303-307.
- 13 J. Cížek, in *Advances in Chemical Physics*, Ed. P. C. Hariharan, Vol. 14 (Wiley Interscience, New York, (1969)
- 14 G. D. Purvis III, R. J. Bartlett, *J. Chem. Phys.* **1982**, *76*, 1910-1918.
- 15 Y. Zhao, D. G. Truhlar, *Theor. Chem. Acc.* **2008**, *120*, 215-241.
- 16 B. O. Roos, P.R. Taylor, P.E.M. Siegbahn, *Chem. Phys.* **1980**, *48*, 157-173.
- 17 C. Angeli, R. Cimraglia, S. Evangelisti, T. Leininger, J.-P. Malrieu, *J. Chem. Phys.* **2001**, *114*, 10252-10264.
- 18 **Reference AVAS**
- 19 F. Weinhold, C. Landis, *Valency and Bonding, A Natural Bond Orbital Donor – Acceptor Perspective*, Cambridge University Press, Cambridge, **2005**.
- 20 K. B. Wiberg, *Tetrahedron* **1968**, *24*, 1083-1096.
- 21 M. J. Frisch, G. W. Trucks, H. B. Schlegel, G. E. Scuseria, M. A. Robb, J. R. Cheeseman, G. Scalmani, V. Barone, B. Mennucci, G. A. Petersson, H. Nakatsuji, M. Caricato, X. Li, H. P. Hratchian, A. F. Izmaylov, J. Bloino, G. Zheng, J. L. Sonnenberg, M. Hada, M. Ehara, K. Toyota, R. Fukuda, J. Hasegawa, M. Ishida, T. Nakajima, Y. Honda, O. Kitao, H. Nakai, T. Vreven, J. J. A. Montgomery, J. E. Peralta, F. Ogliaro, M. Bearpark, J. J. Heyd, E. Brothers, K. N. Kudin, V. N. Staroverov, R. Kobayashi, J. Normand, K. Raghavachari, A. Rendell, J. C. Burant, S. S. Iyengar, J. Tomasi, M. Cossi, N. Rega, J. M. Millam, M. Klene, J. E. Knox, J. B. Cross, V. Bakken, C. Adamo, J. Jaramillo, R. Gomperts, R. E. Stratmann, O. Yazyev, A. J. Austin, R. Cammi, C. Pomelli, J. W. Ochterski, R. L. Martin, K. Morokuma, V. G. Zakrzewski, G. A. Voth, P.

-
- Salvador, J. J. Dannenberg, S. Dapprich, A. D. Daniels, O. Farkas, J. B. Foresman, J. V. Ortiz, J. Cioslowski, D. J. Fox, Gaussian 09, Revision C.01. Gaussian, Inc., Wallingford CT, **2009**.
- 22 a) F. M. Bickelhaupt, E. J. Baerends, *Rev. Comp. Chem.* **2000**, *15*, 1-86. b) L. Zhao, M. von Hopffgarten, D. M. Andrada, G. Frenking, *WIREs Comput. Mol. Sci.* **2018**, DOI: 10.1002/wcms.1345. c) G. Frenking, F.M. Bickelhaupt, *The Chemical Bond. 1. Fundamental Aspects of Chemical Bonding*, p. 121-158, G. Frenking and S. Shaik (Eds), Wiley-VCH, Weinheim, 2014.
- 23 *Computer code ADF2017*, SCM, Theoretical Chemistry, Vrije Universiteit, Amsterdam, The Netherlands, <http://www.scm.com>.
- 24 E. Van Lenthe, E. J. Baerends, *J. Comput. Chem.* **2003**, *24*, 1142-1156.
- 25 J. Krijn, E. J. Baerends, *Fit Functions in the HFS-Method*; Internal Report (in Dutch), Vrije Universiteit Amsterdam, The Netherlands (**1984**).
- 26 M. Menéndez, R. Álvarez Boto, E. Francisco, A. Martín Pendás, , *J. Comput. Chem.* **2015**, *36*, 833-843.
- 27 goldbook.iupac.org/html/D/D01523.html.

Captions and Legends

Figure 1. Schematic representation of carbenes CR_2 in the electronic states $^3\text{B}_1$, $^1\text{A}_1$, $^1\text{B}_1$ and relative energies of CH_2 and CF_2 .

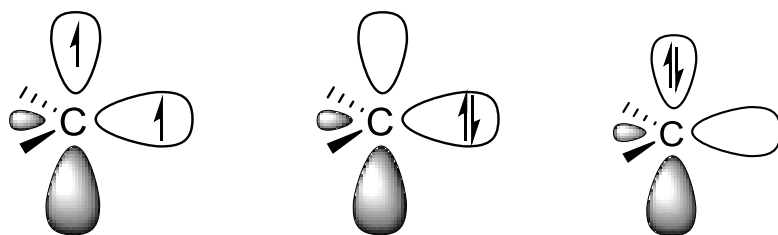
Figure 2. Schematic representation of different types of interactions **A** - **C** in C_2F_4 which are considered in this work. (a) Model **A**, electron-sharing interactions between CF_2 in the electronic excited state $^3\text{B}_1$, (b) Model **B**, dative bonding between CF_2 in the electronic ground state $^1\text{A}_1$. (c) Model **C**, dative bonding between CF_2 in the ground state $^1\text{A}_1$ and the second excited state $^1\text{B}_1$.

Figure 3. Calculated reaction pathway for rupture of the carbon-carbon bond of C_2F_4 with different theoretical methods.

Figure 4. Deformation densities $\Delta\rho$ (isovalues 0.005 au) which are associated with the formation of the carbon-carbon σ and π bonds in (a) C_2H_4 and (b) C_2F_4 . The calculated orbital energies $\Delta E_{\text{orb}}(\sigma)$ and $\Delta E_{\text{orb}}(\pi)$ are taken from Table 4. The colour code for the charge flow is red→blue.

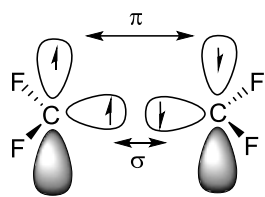
Figure 5. Laplacian of the electron density $\nabla^2\rho$ (isovalues -0.2 au) calculated at the M06-L level at several points of the cleavage reaction. (a) Equilibrium geometry, (b) $\text{R}(\text{C}-\text{C})=1.7 \text{ \AA}$, (c) $\text{R}(\text{C}-\text{C})=3.0 \text{ \AA}$

Figure 6. Two main bonding natural adaptive orbitals between the CF_2 fragments at the M06-L level (isovalues ± 0.1 au). The labeling of geometries is the same as in Figure 5.

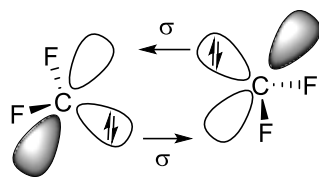


CH ₂	0.0 kcal/mol	9.0 kcal/mol	45.5 kcal/mol
CF ₂	54 kcal/mol	0.0 kcal/mol	155.2 kcal/mol

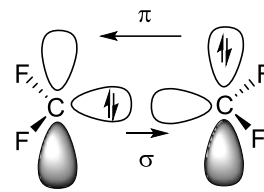
Figure 1



(a) **A**



(b) **B**



(c) **C**

Figure 2

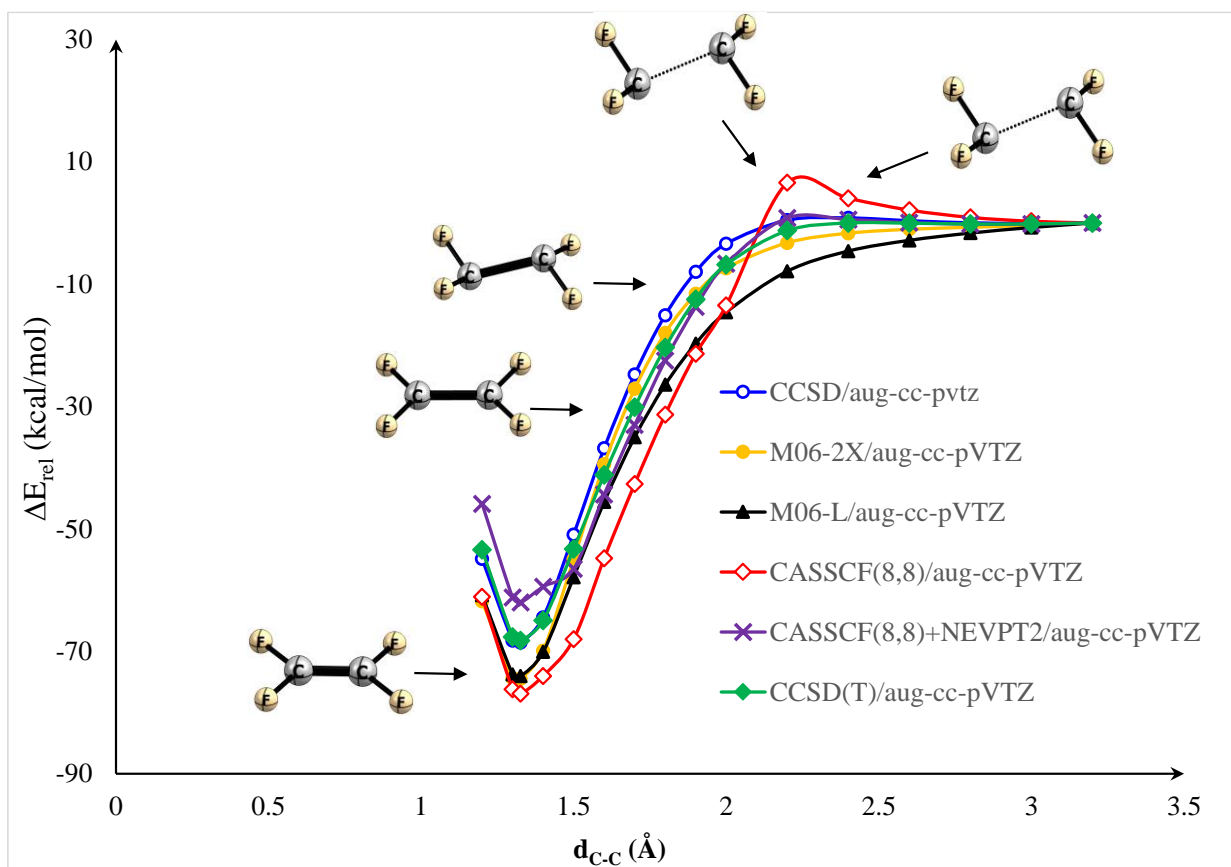
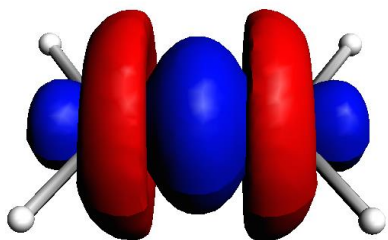
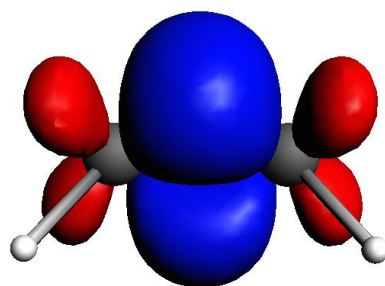


Figure 3

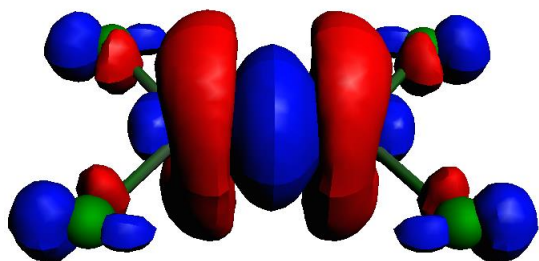


$$\Delta E_{\text{orb}}(\sigma) = -218.0 \text{ kcal/mol}$$

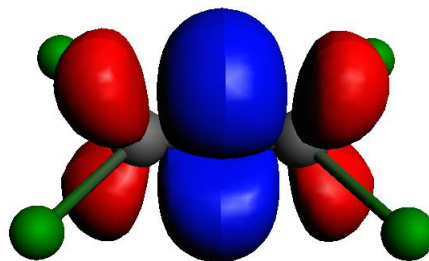


$$\Delta E_{\text{orb}}(\pi) = -79.4 \text{ kcal/mol}$$

(a)



$$\Delta E_{\text{orb}}(\sigma) = -209.2 \text{ kcal/mol}$$



$$\Delta E_{\text{orb}}(\pi) = -87.0 \text{ kcal/mol}$$

(b)

Figure 4

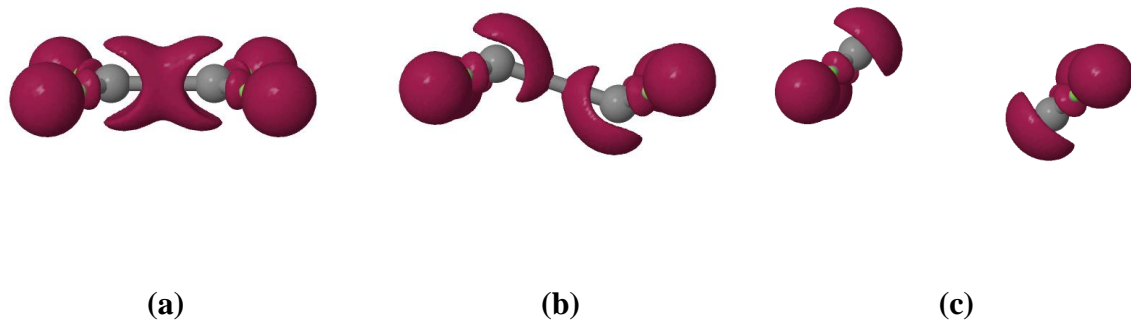


Figure 5

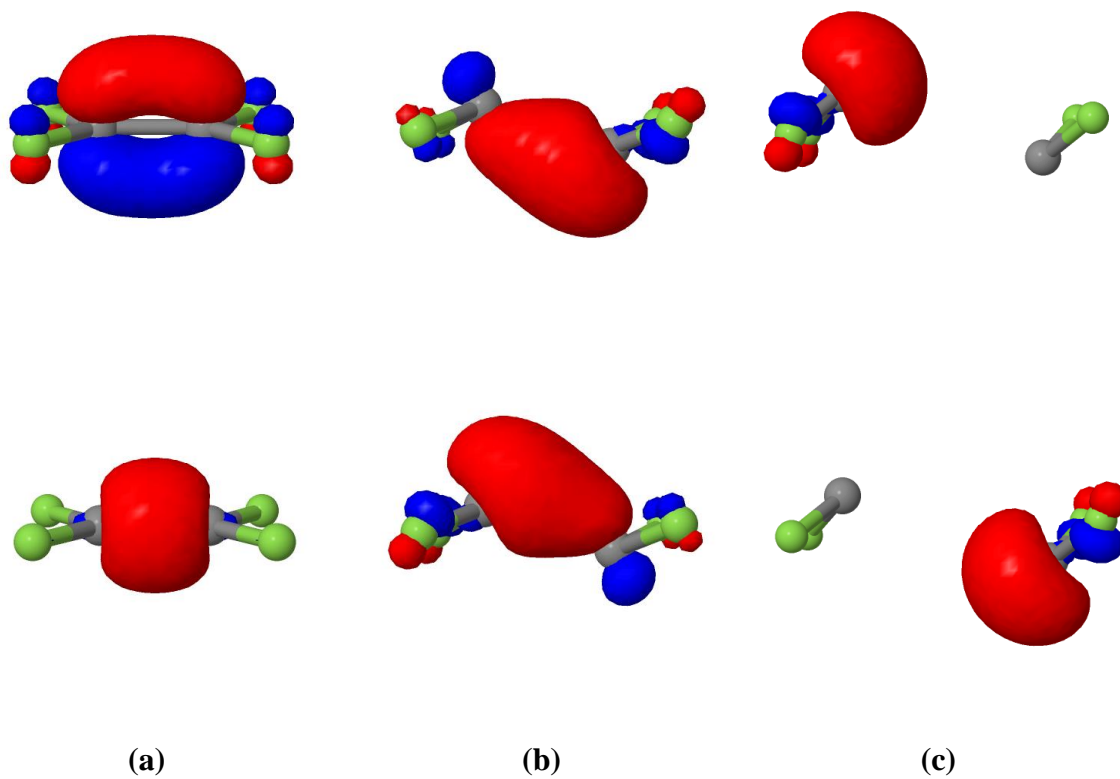


Figure 6

Table 1. Calculated (experimental) C-C bond lengths R_e [Å] and calculated (experimental) bond dissociation energies D_e [kcal/mol]. Calculated values were obtained at the M06-L/TZ2P level of theory.

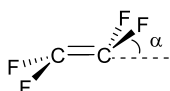
	R_e	D_e
H ₃ C-CH ₃	1.532 (1.522) ^a	93.1 (89.7) ^e
H ₂ C=CH ₂	1.333 (1.336) ^b	178.2 (172.1) ^e
F ₃ C-CF ₃	1.567 (1.545) ^c	87.3 (96.4) ^e
F ₂ C=CF ₂	1.329 (1.311) ^d	73.3 (70.3) ^e

^aRef. 2d; ^b Ref. 2b; ^c Ref. 2c; ^d Ref. 2a; ^eRef. 1.

Table 2. Relative energies [kcal/mol] of C₂F₄ at different C-C distances d_{C-C} [Å] with various theoretical methods relative to the equilibrium bond length (1.326 Å) at M06-L. All calculations employed aug-cc-pVTZ basis sets. Bending angle α of the CF₂ groups.^a

Δd_{C-C}	α	M06-L	M06-2X	CCSD	CCSD(T)	CAS(8,8)	CAS(8,8)PT2
1.20	0.0	13.2	12.7	13.7	14.8	15.8	16.1
1.30	0.0	0.3	0.1	0.3	0.6	0.7	0.8
1.326 ^b	0.0	0.0	0.0	0.0	0.0	0.0	0.0
1.40	0.0	4.0	4.6	4.1	3.3	2.9	2.6
1.50	21.8	16.2	19.5	17.7	15.0	8.9	5.5
1.60	35.0	28.5	35.1	31.8	27.1	22.1	17.7
1.70	43.6	39.0	47.4	43.8	38.1	34.3	29.0
1.80	47.6	47.6	56.5	53.5	47.9	45.6	39.6
1.90	51.1	54.3	62.9	60.6	55.8	55.5	48.3
2.00	53.6	59.5	67.1	65.2	61.4	63.5	55.4
2.20	56.9	66.2	71.3	69.0	67.0	83.5	62.9
2.40	59.0	69.5	72.8	69.4	68.2	81.0	62.6
2.60	60.3	71.2	73.5	69.0	68.2	79.0	62.1
2.80	61.0	72.4	73.8	68.6	68.1	77.9	61.9
3.00	61.0	73.3	74.1	68.5	68.1	77.2	61.9
3.20	61.5	74.1	74.5	68.6	68.2	76.9	62.0

^aThe angle α is defined as:



^bEquilibrium distance

Table 3. Calculated EDA values at M06-L/TZ2P of the orbital term ΔE_{orb} [kcal/mol] for the interactions between CF_2 at with different electronic states and different C-C distances $d_{\text{C-C}}$ [Å]. The red values depict the smallest ΔE_{orb} value at the respective C-C distance.

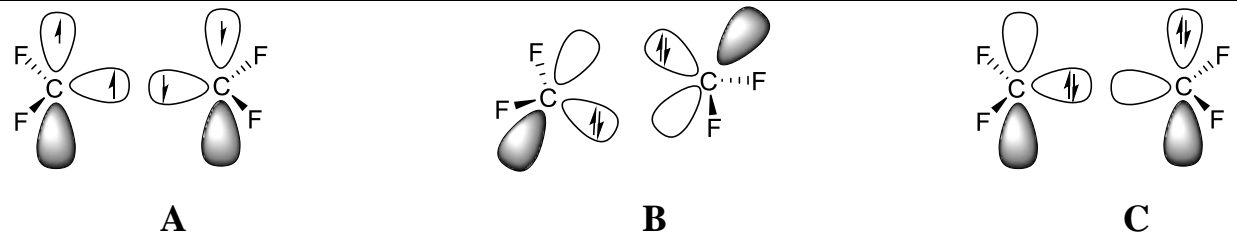
												
$d_{\text{C-C}}$	1.30	1.326 ^a	1.40	1.50	1.60	1.70	1.80	1.90	2.00	2.20	2.40	3.00
	Model A											
ΔE_{orb}	-339.5	-326.1	-290.9	-245.6	-217.3	-195.0	-178.4	-165.9	-156.5	-144.3	-137.7	-131.4
	Model B											
ΔE_{orb}	-856.4	-802.0	-665.8	-420.9	-275.1	-188.0	-133.3	-96.4	-70.4	-38.1	-20.7	-3.9
	Model C											
ΔE_{orb}	-406.0	-392.5	-357.1	-359.4	-365.5	-349.3	-326.1	-303.3	-283.7	-255.0	-237.1	-215.6

Table 4. EDA calculations of C₂F₄ and C₂H₄ at the M06-L/TZ2P level using triplet and singlet fragments according to model **A** and **C** (Figure 2). Energy values in kcal mol⁻¹.

Fragments	C ₂ F ₄		C ₂ H ₄	
	Triplet (A)	Singlet (C)	Triplet (A)	Singlet (C)
ΔE_{int}	-197.7	-279.9	-196.7	-278.1
$\Delta E_{\text{MetaGGA}}$	6.2	-4.8	7.9	7.6
ΔE_{Pauli}	305.0	292.9	291.4	282.8
$\Delta E_{\text{elstat}}^{\text{[a]}}$	-182.7 (35.9 %)	-175.6 (30.9 %)	-183.6 (37.0 %)	-181.2 (31.9 %)
$\Delta E_{\text{orb}}^{\text{[a]}}$	-326.1 (64.1 %)	-392.5 (69.1 %)	-312.4 (63.0 %)	-387.2 (68.1 %)
$\Delta E_{\text{orb}}(\sigma)^{\text{[b]}}$	-209.2 (64.2 %)	-221.5 (56.4 %)	-218.0 (69.8 %)	-241.2 (62.3 %)
$\Delta E_{\text{orb}}(\pi)^{\text{[b]}}$	-87.0 (26.7 %)	-142.0 (36.2 %)	-79.4 (25.4 %)	-129.9 (33.5 %)
$\Delta E_{\text{orb rest}}^{\text{[b]}}$	-29.9 (9.2 %)	-29.0 (7.4 %)	-15.0 (4.8 %)	-16.1 (4.2 %)
ΔE_{prep}	122.2	204.4	20.7	102.1
$\Delta E = -D_e$	-75.5	-75.5	-176.0	-176.0

^aThe values in parentheses give the percentage contribution to the total attractive interactions $\Delta E_{\text{elstat}} + \Delta E_{\text{orb}}$.

^bThe values in parentheses give the percentage contribution to the total orbital interactions ΔE_{orb} .